UNIVERSITY OF CALIFORNIA,
IRVINE

High Frequency Digital Frequency Domain Fluorescence Lifetime Imaging System

THESIS

submitted in partial satisfaction of the requirements
for the degree of

MASTER OF SCIENCE

in Biomedical Engineering

by

Alessandro Rossetta

Thesis Committee:
Professor Enrico Gratton, Chair
Professor Frithjof Kruggel
Assistant Professor Jered Haun

2016

DEDICATION

To my *family*

TABLE OF CONTENTS

LIST OF FIGURES

LIST OF TABLES

ACKNOWLEDGMENTS

Firstly, I would like to express my sincere gratitude to my advisor Prof. Enrico Gratton for the continuous support during studies and related research, for his patience, motivation, and immense knowledge. Besides my advisor, I would like to thank the rest of my thesis committee: Prof. Frithjof Kruggel and Prof. Jered Haun for their advices and encouragement.

My sincere thank also goes to Ylenia Santoro, Milka Titin and Leonel Malacrida: without their precious support it would have not been possible to conduct this research and finish my project.

I thank my fellow labmates Rupsa Datta, PerNicklas Hedde and Suman Ranjit for all the fun we have had in the last two years. I would like also to thank Alexander Dvornikov and Hongtao Chen. Last but not the least, I would like to thank Tracey Scott and Prof. Michelle Digman.

ABSTRACT OF THE THESIS

High Frequency Digital Frequency Domain Fluorescence Lifetime Imaging System

By

Alessandro Rossetta

Master of Science in Biomedical Engineering

University of California, Irvine, 2016

Professor Enrico Gratton, Chair

A system and method is provided for improved fluorescence lifetime measurement. A high frequency digital heterodyning technique is described in which photon counting mode detectors are sampled at a rate slightly slower than a digitally pulsed excitation signal. A digital mixer produces a difference frequency which contains the same information than the high frequency signal. This lower frequency is still suitable for fluorescence lifetime measurements in microscopy. The digital algorithm provides phases and modulations of detected photons binning them into phase steps and time windows. The digital heterodynig algorithm was implemented in a very low cost FPGA (Field Programmable Gate Array).

Chapter 1

Introduction

When a fluorescent molecule is excited by an external source, the time distribution for when the stored energy is released, under the form of a photon, has the shape of an exponential decay of the form $e^{-t/\tau}$, where τ represents the lifetime of the fluorophore. So basically we define fluorescence lifetime the average amount of time it takes to a molecule to go back to its ground state after it has been excited. It is known that the lifetime of a fluorophore can be sensitive and consequently modified by the chemical environment and or the proximity of other molecules. This particular property can be used to perform quantitative analysis of molecular structures, chemical environments, and biological systems based on the decay time. Fluorescence lifetime has another important property, i.e. it is independent of the total amount of fluorescence that is why fluorescence lifetime can be used as a measuring tool independently of fluorophore concentration, efficiency of detector and intensity of the illumination source used for excitation (Robert M. Clegg, Peter C. Schneider, 1996).

The determination of the lifetime of the excited state is a widely used technique to characterize fluorescent molecular species. In the field of fluorescence microscopy, fluorescence lifetime imaging (FLIM) can provide a new contrast mechanism to help identify the local fluorophore environment. Among the most common applications of FLIM we have the determination of ion or other small ligand concentration using lifetime-sensitive dyes, the determination of oxygen concentration in cells and the calculation of

Föster resonance energy transfer (FRET) for distance measurements in the nanometer scale.

Among the techniques used for fluorescence lifetime and FLIM calculation there are two main methods to obtain the fluorescence lifetime: Time-Correlated Single Photon Counting (TCSPC) and Frequency Domain phase-modulation. Both techniques provide substantially the same information and differ mainly and only in how the time-resolved fluorescence data are acquired and calculated. TCSPC is a Time domain (TD) technique versus phase-modulation which is a Frequency domain (FD) approach (Spencer, R.D., G.Weber, 1969).

The time domain method it is based on constructing the histogram of photon delays using the time-correlated single-photon counting method: TCSPC determines fluorescence lifetime by measuring the arrival time of each detected photon with respect to the previous laser pulse. This operation is commonly done with a sub-nanosecond precision by using an expensive and slow time-to-amplitude converter (TAC) or time-to-digital converter (TDC). The standard of precision for this approach turns out to be very high and each photon is collected with the same level of uncertainty (Becker, 2004).

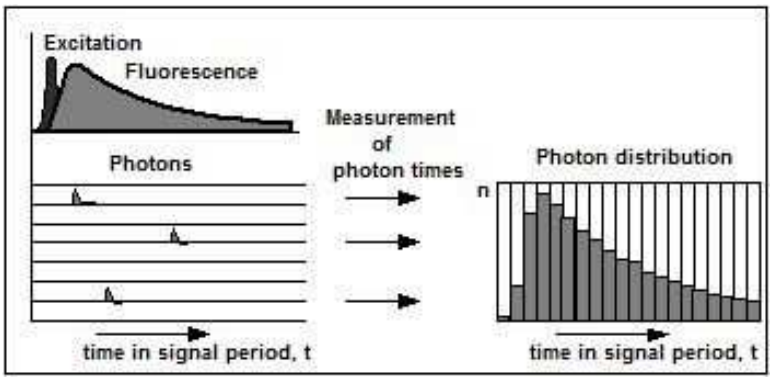

Figure 1.1 – TCSPC principle: photons are collected after laser excitation and the fluorescence decay histogram is built by binning the photons depending on their arrival time.

The frequency domain method consists of measuring the harmonic response of a fluorescent system using either a sinusoidal modulation of the excitation light or a fast repetition pulse train laser.

1.1 TCSPC versus FD

Frequency domain and time domain techniques of measuring fluorescence lifetime decay have been previously and widely discussed, but here we propose an overview of the key points of both of the methods.

From the statistics point of view the uncertainty of the TCSPC measurement ultimately depends on the number of photons collected which is considered the minimum error possible. Also the dark noise, which are photons detected but not correlated with the decay, are minimal in TCSPC.

However, the total number of photons collected in the TCSPC is not maximal. The TCSPC technique based on the TAC (time to amplitude converter) approach has a relatively large dead time and poor duty cycle which depends on the method used to measure the delay between the laser and the detection of a photon. Furthermore, when used in conjunction with high repetition rate lasers, which is the norm today, the entire laser period cannot be measured unless the duty cycle is reduced (Gratton, 2003).

Talking about frequency domain methods, every time a photon is detected by the system, the modulated detector photocurrent that is generated it is directly used without the need of a discriminator, avoiding dead time and possibly detecting all photons including the dark counts from thermal emission of the dynodes. In the classical FD approach the detection and data processing is done in the analog mode and then the signal is converted in digital form after filtering for the desired light modulation frequency. A common criticism of the frequency domain method is that the FD system operates at a single frequency and it cannot resolve very short lifetimes. A second criticism is that the duty cycle is 50% or lower due to the modulation of the gain of the detector. A typical use of the frequency domain method is for cases where the photon flux is very high, in these applications the time-domain method cannot keep up (Gratton, E., D.M. Jameson, R.D. Hall, 1984).

From the mathematical point of view, the time domain or the frequency domain analyses of periodic signals are equivalent, being related by the Fourier transform. Therefore the differences

between the two methods are a consequence of the way data are collected and processed rather than due to any profound reason.

Frequency domain measurements are based on the calculation of the phase shift ϕ and modulation *m* between the excitation and the emission signals (see Figure 1.2)

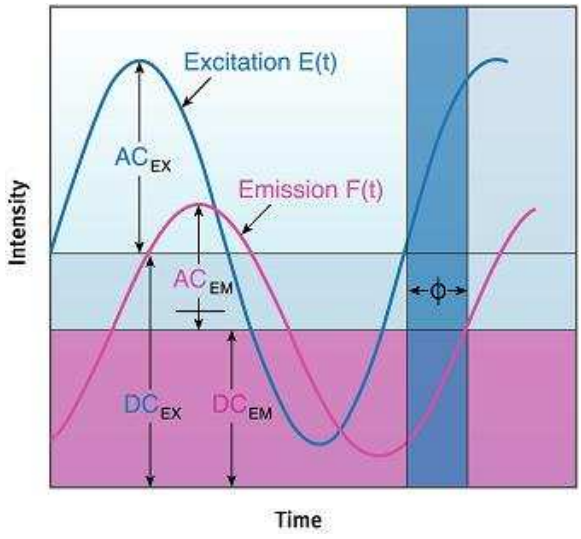

Figure 1.2 – Frequency domain principle: E(t) is the Laser light while F(t) represents the emitted light from the sample. Φ represents the phase shift between the two waves and the modulation *m* can be obtained with the ratio: $m = [(AC/DC)_{em} / (AC/DC)_{ex}]$

It is possible to calculate the fluorescence lifetime from phase shift and modulation according to the following formulas:

$$\tau_{p,h} = \frac{1}{2\pi h f_{ex}} \tan(\phi_{F,h})$$

$$\tau_{m,h} = \frac{1}{2\pi h f_{ex}} \sqrt{\frac{1}{m_{F,h}^2} - 1}$$

A great advancement in frequency domain approach was introduced when the first "cross-correlation" instrument was developed in which detection of the phase shift and of the modulation ratio was performed using the heterodyning or cross-correlation principle. Since it is technically difficult to measure the phase and modulation at very high frequencies (160MHz in the first applications), the high frequency, at which the measurement is performed, is down converted to a very low frequency: the cross-correlation frequency (Spencer, R.D., G.Weber, 1969). In this implementation of the technique, the detector gain was modulated at a frequency which is slightly different from the frequency used to modulate the light source. Because of the detector gain modulation, this approach provided a maximum duty cycle of 50%. The gain modulation produces a difference frequency which is filtered and digitized for accurate phase and modulation determination.

However, one limitation of these early instruments was that complex exponential decays could not be resolved using only one or two light modulation frequencies. This explains the interest in developing the frequency domain technique but for multiple modulation frequencies.

The implementation of the cross-correlation method is achieved by generating two frequencies, one used for the modulation of the intensity of the light source at a frequency f and a second frequency at $f + \delta f$ used to modulate the gain of the detector where δf is in the 10 to 1000Hz

range. The detector in this case acts as a mixer by multiplying the signals at these two frequencies. The two signals are the modulated light impinging on the detector and the voltage used to modulate the gain of the detector. The output current of the detector is proportional to the light intensity times the gain of the detector. The product of two frequencies gives the sum and the difference of these frequencies. The sum is at very high frequency and it can be filtered from the difference δf using low pass frequency filters (Gratton, E., et al., 1984). Only the difference frequency is used – Figure 1.3.

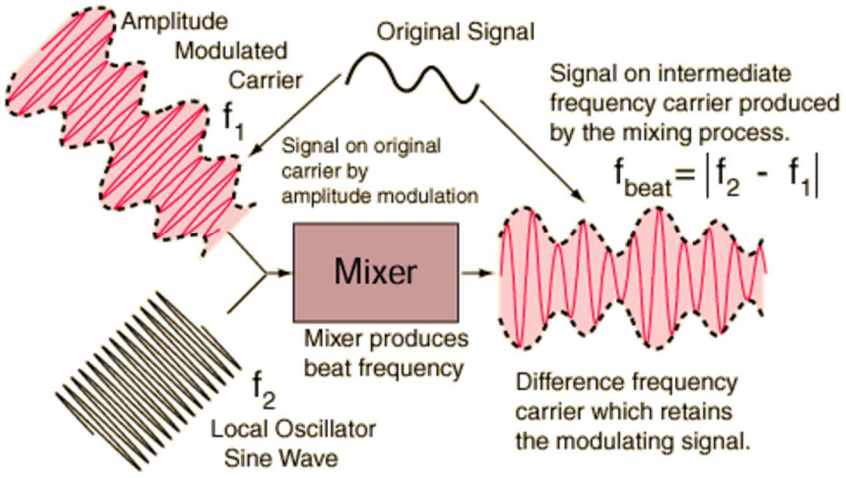

Figure 1.3 – Heterodyning principle example: if we consider f_2 the laser frequency and f_1 the frequency coming from the detector in a way that $f_2 = f_1 + \delta f$, then f_{beat} corresponds to the cross-correlation frequency where $f_{beat} = \delta f$.

The downsides of the classical frequency domain approach have been bypassed by the FLIMBox approach which is an electronic circuit for producing the frequency representation of the fluorescence decay (Colyer, R.A., C. Lee, E. Gratton, 2008). As it was described in the previous section, the conversion from the high frequency of the source repetition to the low frequency of the

measurement is produced by the heterodyning process in which the output current of the detector which is at the frequency of light modulation is mixed (multiplied) by a slightly different frequency. If instead of using a sinusoidal signal to modulate the gain of the detector a narrow pulse is used (Feddersen, B.S.,D.W. Piston, E. Gratton, 1989)i.e. a signal which contains many harmonics, the multiplication generates not one, but a spectrum of harmonics that is the replica of the spectrum at high frequency.

In the FLIMBox method narrow pulses, called windows, are also used so that multiple frequencies are measured in parallel with a duty cycle of 100% using a Digital Frequency Domain (DFD) heterodyning method.

Digital heterodyning technique – Figure 1.3 -, which consist in a pure mathematical algorithm and will be discussed later, was developed to achieve 100% duty cycle, so that no photons are lost, and to have a higher harmonic content compared to the classic frequency domain approach. DFD offers the possibility to be used with typical photon detectors and commercial laser scanning microscopes, it has very high performance (comparable to TCSPC's level of precision) at very low cost because DFD was conceived to work on an FPGA – Field-Programmable Gate Array – platform: the price for FPGA chip is around or below 50$ – FPGAs were also chosen for their reprogrammability and parallel acquisition capabilities (N.P. Barry, J. Eid, E. Gratton, 2003) . A mathematical model of DFD shown that DFD and TCSPC methods have the same statistical accuracy.

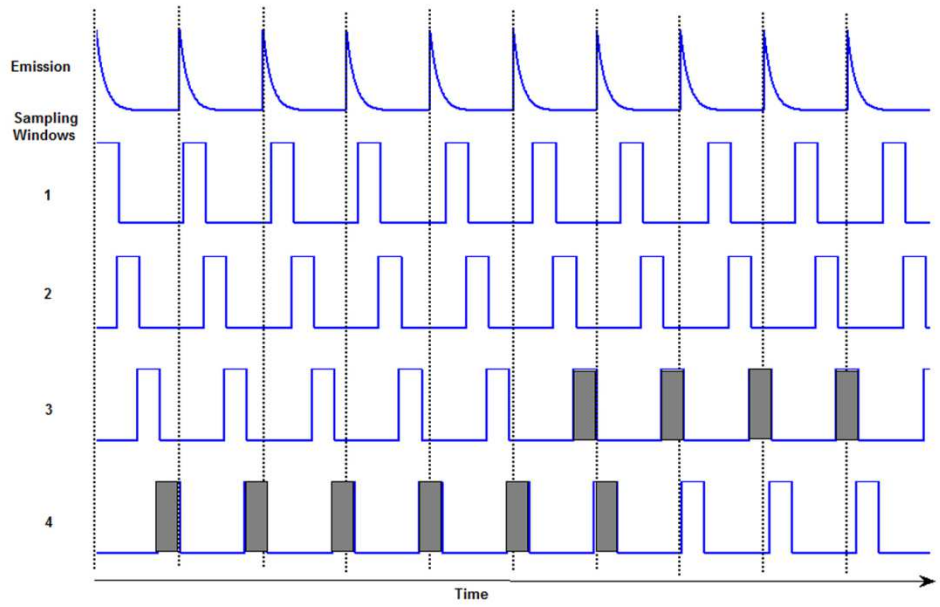

Figure 1.4 - Digital heterodyning principle: arriving photons are assigned to one of four sampling windows (exaggerated example) according to their arrival time. In the real case, the sampling windows slide through the entire period of the emission response due to the slight difference in frequencies, for a total of 256 steps.

Talking about the construction of the decay histogram, the TCSPC and the FLIMBox essentially provide the same results but with some technical differences. In the TCSPC the time axis is divided in time bins typically 1024 time channels or more. In FLIM microscopy, due to the limited number of photons collected per pixel, the number of channels is generally reduced to 256 or 128 since the total counts per pixels is no more than 1000 counts/photons.

The concept of dividing the photons time of arrival in bins is also used in the FLIMBox, where the laser repetition period is divided in 256 phase intervals, but synchronized with the period of the laser – Figure 3.1.

So the basic difference between the FLIMBox and the TCSPC is the way the time bins are generated. In the FLIMBox, the time bins are derived by division of the laser repetition period. In the TCSPC the time bins are produced independently of the laser rep rate as they are determined by sampling a linear ramp using the TAC principle.

Other main differences are the dead time for data processing, the time resolution and the duty cycle. The dead time of the FLIMBox technique is due to the discriminator rather than the internal FLIMBox circuit. The TCSPC dead time depends on the recovery time of the TAC. According to manufactures specifications, both PicoQuant and B&H quote figures in the order of 100-120ns dead time, depending on the model of their data acquisition card. At high counting rates, this large dead time can strongly affect the linearity of the data collection in terms of time and intensity linearity.

TCSPC time resolution refers to the pulse-to-pulse separation, this is true since the TCSPC uses a very small bin time. However, in the case of a fluorescence lifetime, which is an exponential process, photons are necessarily spread among bins. In this case the time resolution depends primarily on the number of photons collected in the decay curve. The FLIMBox is very efficient and maximize the information from the photons collected.

Lastly, talking about the duty cycle, the FLIMBox is always active, so that photons are collected irrespective of their time of arrival. In the TCSPC the time axis is limited to a percentage of the total period of the laser pulse.

The following table shows the evolution and the state of the art of frequency domain lifetime instrumentation developed at LFD (Laboratory for Fluorescence Dynamics).

Table 1.1 – Evolution of FD instrumentation at LFD

Parallel fluorometer (1986)	Digital Mixing (2000)	First FLIMBox (2007)	Parallel- FLIMBox (2009)
Analog mixing with pulsed external generator. Mixing using the detector gain	Digital mixing with external square wave generator. Detector gain not modulated	Digital mixing. Internal generator modulate signal after detector @ 48MHz	Digital mixing. Internal generator produce pulsed modulating signal @ 10, 20 MHz.
Duty Cycle depends on harmonics. 6% for n=16	Duty Cycle is 50%.	Duty Cycle is 100%	Duty Cycle is 100%
Parallel frequency domain lifetime instruments	FCS. System not ready to implement parallel acquisition	FLIM. System not ready to implement parallel acquisition	Parallel Digital Frequency domain for cuvette, FLIM, and FCS.
One input channel	One input channel	Two input channels	Up to four input channels
Average acquisition time takes several minutes			Average acquisition time takes seconds
		Frame synchronization and saturation problems. Limited number of windows, design instable	Flexible synchronization. Saturation control. 8 and 16 windows available. Stable design

Considering what has been said so far the goal of this project was to bring the 2009 FLIMBox version into another era by overcoming the bottlenecks of the previous instrument. With the introduction in the market of very inexpensive digital electronics available in the current FPGA chips it is possible to build a much higher performances device with less than 50$. The aims of the new FLIMBox were to increase the maximum modulation frequency for the detector to achieve even higher harmonic content, to improve data transmission rate and, due to the presence of new multi-channel detectors, to implement a multi-channel instrument with the capability of acquiring and processing more than four channels at the same time. The design we propose was developed using a completely new and more modern approach to digital electronics that allows the instrument itself to be mold for different applications ranging from microscopy, FLIM, FCS and tissue imaging.

1.2 The FLIMBox

Digital Frequency Domain with FPGA implementation has already reached the market with a product called FastFLIM sold and produced by ISS Inc Champaign, Illinois. The FastFLIM is the evolution of an instrument previously developed at Laboratory for Fluorescence Dynamics (LFD) by Dr. Ryan Colyer called FLIMBox – Figure 1.2 – but several issues regarding the actual implementation and design of the instrument in the FPGA chip have not been fixed yet. The current design from 2009 has a dead time of 3ns which means that photons can be sampled continuously due to 100% duty cycle but only every 3 ns because the narrow pulses that sample the incoming light are generated using a 320MHz frequency. This feature drastically reduces the harmonic content of the sampled light cutting a piece of information that is extremely relevant in frequency domain applications.

Another important limitation that the 2009 version has is that data transmission is limited by the USB chip latency used in the current electronic board. Large USB latency makes FPGA internal memory (FIFO – First In First Out) to overflow and photons to get lost during USB recovery time. Every time there is an internal overflow, photon acquisition goes in a standby mode forbidding the incoming photons to be sampled.

FIFO memory is important because this method of storing photons allows to organize and manipulate data according to time and prioritization. In essence, the queue processing technique is done as per first-come, first-served behavior. The algorithm data

reconstruction builds photons history according to the order they comes. Each photon is stored in a queue data structure. The first data which is added to the queue will be the first data to be removed. So if this process has any leaks data reconstruction will be impossible especially in those applications where a large amount of photons, 10 million counts per channel (tissue biospectroscopy), have to be collected.

The USB chip used in the old FLIMBox is the FX2 from Cypress (Cypress, San Jose, CA,USA). This chip can only transmit data at rate of 12MHz with a width of 16bit, in other words only few information regarding the photons can be transmitted to the computer for data processing, limiting enormously the maximum number of parallel channel that is possible to acquire at the same time; in the current design only four channels can be represented.

Moreover the circuit of old FLIMBox has been implemented in a FPGA chip using a schematic programming language. The circuit is first virtually created in the FPGA programming environment under the form of a drawing, by actually connecting the different components with wires, and then downloaded into the chip. This "circuit schematic" approach is now substituted by a newer implementation method which consist of writing an actual code in a programming language called VHDL. VHDL was therefore used in this master thesis project to design the new FLIMBox.

Figure 1.5 – The first FLIMBox ever produced at ISS (2007)

1.3 Field Programmable Gate Arrays - FPGAs

The main purpose of this thesis was to design a newer generation of FLIMBox capable to overcome the problems of DFD circuit design related to photon acquisition and processing present in current instrumentation. The method used to reach this goal was the implementation of DFD algorithm using VHDL – VHSIC Hardware Description Language. Instead of drawing the circuit schematic, with VHDL it is possible to code the behavior of an electronic circuit that needs to be synthetized in the FPGA. What is an FPGA? FPGAs are semiconductor devices composed by a matrix of configurable logic blocks (CLB) connected via programmable switches. Using prebuilt logic blocks and programmable routing resources, these chips can be configured to implement custom based hardware functionality without ever using a soldering tool – Figure 1.3.

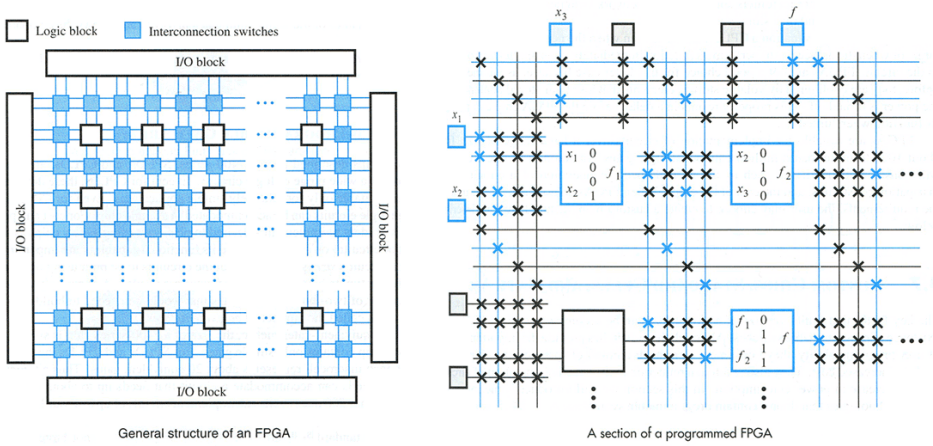

Figure 1.6 – FPGA architecture

It's possible to develop digital computing tasks in VHDL software (using ISE compiling software from Xilinx), simulate their behavior and compile them down to a configuration file or bitstream that contains information on how the CLBs should be wired together. The VHDL code can be considered more a firmware than software. In addition, FPGAs are completely reconfigurable so they can be reprogrammed with other firmware.

FPGAs provide hardware-timed speed and reliability. Reprogrammable silicon also has the same flexibility of software running on a processor-based system, but it is not limited by the number of processing cores available. Unlike processors, FPGAs are truly parallel in nature, so different processing operations do not have to compete for the same resources. Each independent task is assigned to a dedicated section of the chip, and can function autonomously without any influence from other logic blocks. As a result, the performance of one part of the application is not affected when more processing is added (Arnesano, 2013).

Chapter 2

DFD Hardware Implementation

As it was previously said, the classical frequency domain approach modulates the gain of a photomultiplier tube, which acts as a mixer to produce the heterodyning frequency. In Digital Frequency Domain the mixing process is performed using multiple sampling windows generated at a slightly different frequency from the laser repetition rate resulting in the generation of the equivalent of the heterodyning as shown in Figure 2.1.The sampling windows are "narrow pulses" internally generated by the instrument to sample the incoming photons, whenever a photon gets detected the FLIMBox assigns a window number w_{arr} to it. In this way the signal from the detector i.e. the photons, can be processed by an arbitrary number of sampling windows without any loss of signal (Digital frequency domain heterodyning has 100% duty cycle) keeping the PMT "on" for the entire length of the measurement (Colyer R. A., 2008). While in the classical frequency domain method modulating the PMT to produce mixing meant switching "on" and "off" the detector according to a sinusoidal law, of course when the PMT was "off" no photons could be registered and therefore are lost.

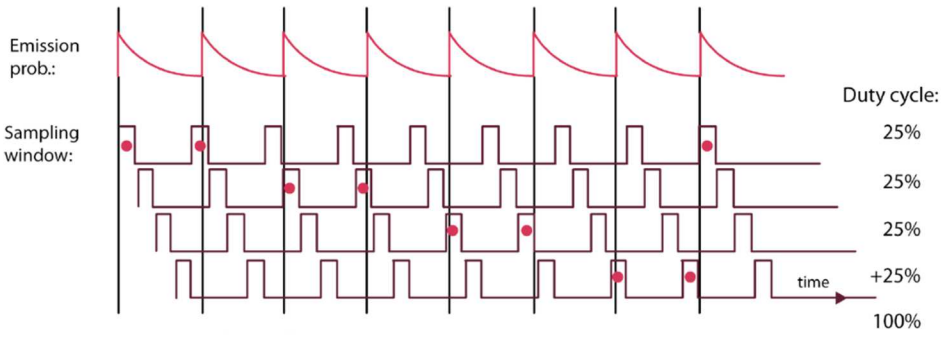

Figure 2.1 - DFD principle with 100% duty cycle, with exaggerated heterodyning such that $f_{cc} = f_{ex}/8$ instead of $f_{cc} = f_{ex}/256$ which we used in our implementation. Photons – represented in the image as dots – are binned into one of the four sampling windows according to their arrival time.

The heterodyning principle is still used in this digital implementation by generating the sampling windows (Figure 2.2B) – PMT modulation frequency in the classical FD approach – from the laser frequency (Figure 2.2A). The heterodyne technique allows translating the fluorescence frequency, which is a relatively fast phenomenon in the order of nanoseconds (Gigahertz), into a cross-correlation phase histogram by creating a slower frequency (in the Megahertz) replica of the fluorescence decay in the microsecond time unit - Figure 2.2C.

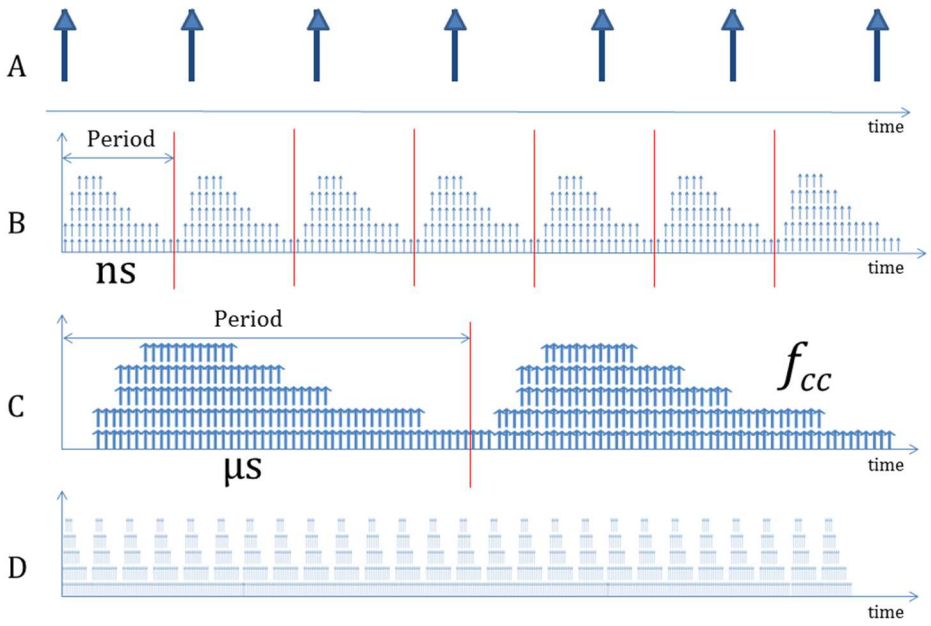

Figure 2.2 – Heterodyning principle summary: A - Laser frequency represented as laser pulses. B - Modulation frequency period and fluorescence lifetime decay drawing. C - Cross correlation frequency signal as a result from the difference between laser and modulation frequencies. D - Cross correlation frequency signal due to the sum of laser and modulation frequency.

For this thesis a newer version of the FLIMBox was created: the DFD algorithm is implemented in VHDL code on a SPARTAN 6 Xilinx FPGA. The specific hardware used was a Xilinx SP601 (San Jose, CA, USA) development board together with a Cypress SuperSpeed Explorer Kit – FX3 USB 3.0 (San Jose, CA, USA) for PC data transfer. The FPGA contains four digital clock managers (DCMs) but, compared with the 2009 FLIMBox in which 3 DCMs were utilized; only two DCMs are used in this new design. A substantial advantage of the new design is the different use of the DCMs which allowed extending the frequency of operation of the device to the Gigahertz range. Another advantage is that the throughput is improved by a large factor because of the availability of the USB protocol in the new board.

Digital electronic circuit and especially those digital circuits in which periodic signals are generated and then used, are affected by special type of noise called *jitter*. Jitter noise is defined as the deviation from true periodicity of a presumed periodic signal. In our application where high frequencies are involved and high precision for photon window determination is needed, jitter noise is crucial matter and has to be controlled and reduced as much as possible. In fact jitter can significantly affect lifetime fluorescence measurements by "moving" in time the generated windows and changing thus the shape of the phase histogram.

That is why we have chosen only two DCMs in a cascade configuration (Figure 2.3): to minimize the amplification of jitter throughout the process of frequency synthesis which will be discussed in the next paragraph.

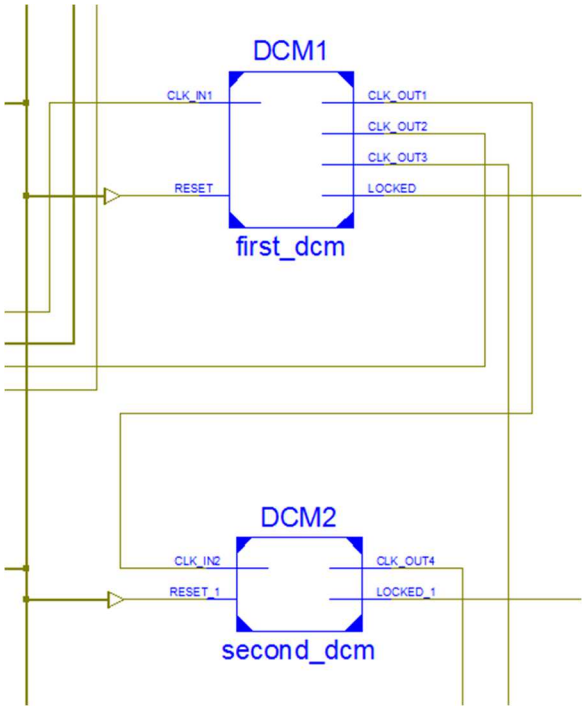

Figure 2.3 – DCMs cascade for jitter minimization

DCMs provide clock synchronization to an external Laser clock and clock multiplication services. Each DCM (DCM SP primitive VHDL component for SPARTAN 6) multiplies and divides the laser input clock frequency by n_d/m_d, where n_d and m_d are integers ranging from 1 to 32. To implement the heterodyning principle in a digital system, it is convenient to have a cross-correlation frequency which is a whole integer fraction of the sampling frequency, f_s. In our case the resulting sampling frequency and cross-correlation frequency of $f_{cc} = f_{ex}/256$, are given by:

$$f_s = \frac{255}{256} f_{ex}$$

$$f_{cc} = \frac{f_{ex}}{256}$$

For 80MHz excitation frequency coming from a Mai Tai Laser, with the use of only two DCMs, an 8X clock is generated at 637.5MHz – the second DCM is using a Phase Locked Loop (PLL) circuit - providing the heterodyning frequency of 79.6875MHz and correspondingly, a cross-correlation frequency of 312.5KHz which means that the phase histogram will have a period of 3.2μs so the fluorescence decay is slowed down by a factor of approximately 10^3. The 637.5MHz clock window frequency, which corresponds to our sampling 1.568ns narrow pulses, is then used as the input for a digital counter which tags incoming photons assigning them a sampling window number (0 to 7) depending on their arrival time – 8 windows are generated within the sampling frequency period. To relate the window during which a photon arrived to a portion of the laser excitation period, it is necessary to know the relative phase difference between the sampling and excitation clocks. A cross-correlation phase counter which runs at Laser clock speed provides measurements of the relative phase difference between the sampling and excitation clocks during each sampling period. The circuit then, as soon as a photon as detected, writes the arrival window, w_{arr}, and the cross-correlation counter value, p_{cc}, for each photon count into a FIFO memory. These two values (w_{arr} and p_{cc}) can be combined into a cross-correlation phase bin number according to the formula:

$$p = 255 - \left[\left(p_{cc} - \frac{256 w_{arr}}{n_w}\right) mod 256\right]$$

where n_w is the total number of sampling windows. The cross-correlation phase bin number is used to construct the cross-correlation phase-histogram $H_{(p)}$ which give us the profile of the fluorescence lifetime decay binned into 256 steps. So the output of the digital circuit carries two important parameters: one is the window that gated the photon acquired, the second is the position of this window in the 256 possible phase shifts positions between laser frequency and sampling frequency, i.e. the phase bin. These two parameters are processed by a computer through a software built at the LFD (SimFCS) to generate a cross-correlation phase histogram, which basically corresponds to the same histogram of photons arrival times (delays) obtained by TCSPC.

2.1 System Design and Layout

The new FLIMBox was installed in a Zeiss Axiovert S100TV microscope with Spectra-Physics MaiTai HP Laser and in the DIVER microscope (Gratton, Dvornikov, & Crosignani, 2014) equipped with a MaiTai Laser too. The instrument was connected to both microscopes following the schematic shown in Figure 2.2. In this setup we used the Mai Tai Laser CLOCK OUT frequency to synchronize FLIMBox's window and phase counter clock frequencies. A scan enable control line was included in the firmware logic control allowing the scanner mechanism to signal when each frame or line has started.

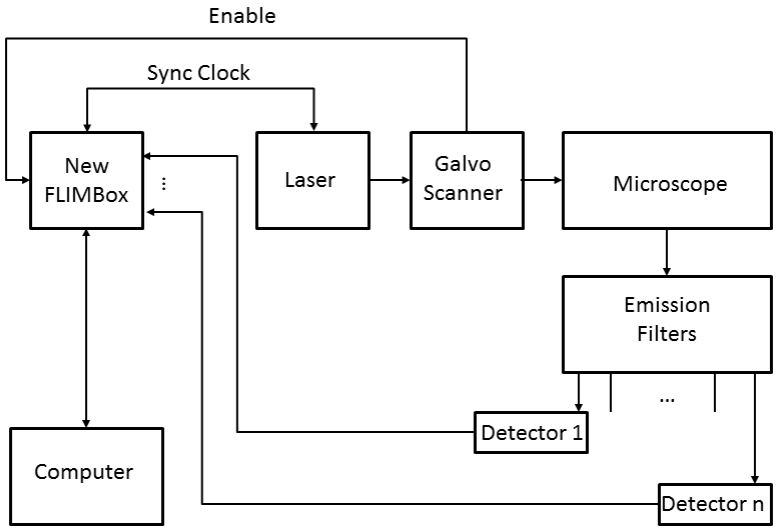

Figure 2.4 – Experimental setup for the new FLIMBox

Photon counts were directly fed into the FPGA chip (Xilinx development board SP601 - Figure 2.5A) for processing, and sent out to the computer for analysis via the Cypress SuperExplorer FX3 development board (Figure 2.5B).

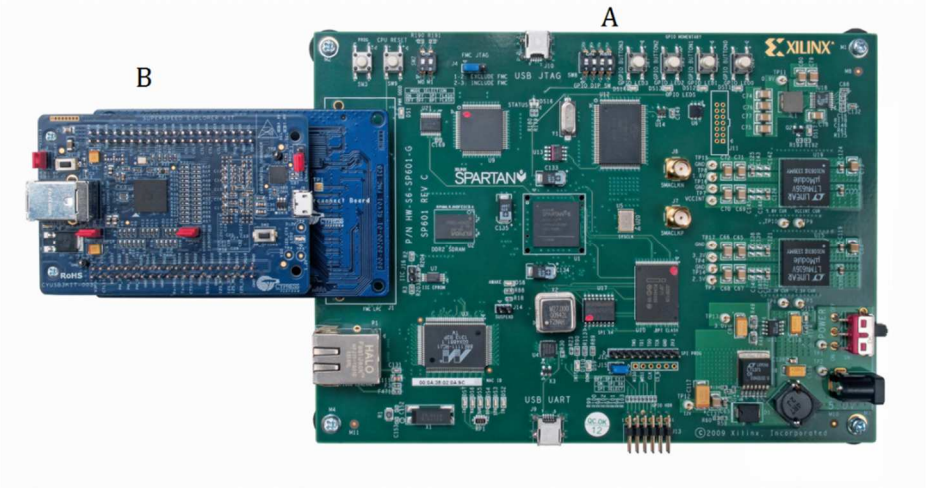

Figure 2.5 – FLIMBox hardware core composed by Xilinx SP601 (A) and SuperSpeed Explorer Kit (B)

Once the FIFO data are read by the computer, the cross-correlation phase histogram at each pixel, $H_{(p)}$, is then constructed by SimFCS software for the FLIM analysis. It is possible to obtain the intensity image by summing the n_p points of the phase histogram for each acquired pixel according to the formula where N is the total number of photon:

$$N = \sum_{p=0}^{n_p-1} H_{(p)}$$

2.2 Phasor calculation and graphical representation

The phasor method transforms the phase histogram of the time delays at each pixel in a phasor (a vector in phase space) – Figure 2.6. The values of the sine-cosine

transforms are represented in a polar plot as a two-dimensional histogram (phasor plot). Each pixel of the image gives a point in the phasor plot. The phasor plot is also used in a dual mode in which each data point of the phasor plot can be mapped to a pixel of the image. Since every molecular species has a specific phasor, we can identify molecules simply by their position in the phasor plot (Digman M.A., Caiolfa V.R., Zamai M., Gratton E., 2008).

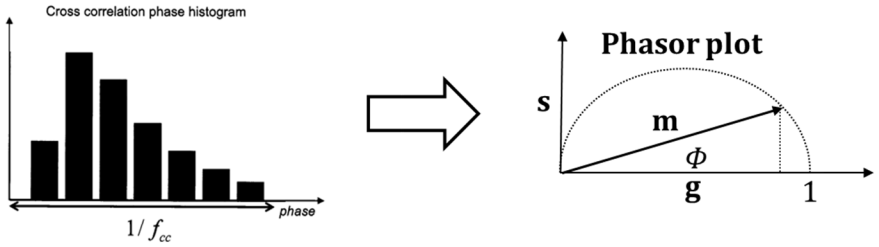

Figure 2.6 – Phase histogram to phasor plot transformation concept

The phasor approach is a method for graphically representing phase and modulation data for FLIM data, the phasor coordinates g and s are – see Figure 2.6 – determined for each harmonic h of the phase histogram as follows:

$$g_{H,h} = \frac{1}{N} \sum_{p=0}^{n_p-1} H_{(p)} \cos(2\pi hp/n_p)$$

$$s_{H,h} = \frac{1}{N} \sum_{p=0}^{n_p-1} H_{(p)} \sin(2\pi hp/n_p)$$

where N is the total number of photons and n_p is the number of bins in the phase histogram. From these two terms, the phase and modulation values are calculated according to the vector transformation equations:

$$\phi_{H,h} = \tan^{-1}\left(\frac{s_{H,h}}{g_{H,h}}\right)$$

$$m_{H,h} = \sqrt{g_{H,h}^2 + s_{H,h}^2}$$

The g and s values are plotted as shown in Figure 2.7.

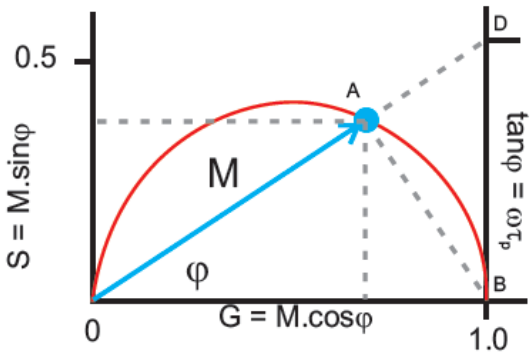

Figure 2.7 - Phasor plot representation

Chapter 3

Result and data analysis

In this chapter the measurements performed to characterize and fully present the capabilities of the new version of the FLIMBox are reported. In particular we will describe the circuit components that we have implemented and we will show electronic tests performed to evaluate the frequency response of the new electronics and for the measurements of fluorescence lifetime in calibration solutions and complex samples such as *Convallaria majalis* and Urea crystals to show also how the new FLIMBox can be integrated in current microscope setups available in our lab.

3.1 The new FLIMBox

As we discussed, the circuit of the new FLIMBox is a firmware and not a schematic anymore. In order to describe in an intelligent way and better understand what has been done we will present the register-transfer level (RTL) of the schematic. ISE software from Xilinx in facts, gives the user the possibility to visualize the VHDL code in a circuit schematic way called RTL. The RTL is a design abstraction which models a digital circuit in terms of the flow of digital signals (data) between hardware registers,

and the logical operations performed on those signals. A simplified version of new FLIMBox RTL is shown in Figure 3.1.

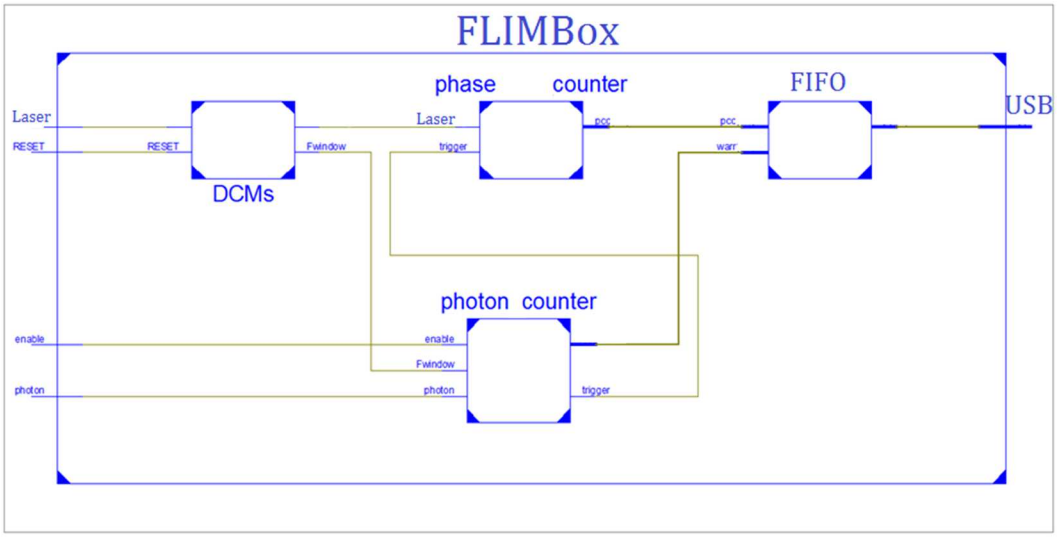

Figure 3.1 – Simplified RTL of the new FLIMBox

By looking at Figure 3.1 it easy to identify the different components implemented. On the left and right sides input and output signals are listed. In this schematic, we show the DCMs (Figure 2.3) module in which frequency synthesis is performed starting with the laser frequency. Two frequencies are generated, one is the replica of the laser frequency and the other is the heterodyning frequency. We can also see how the signals generated by the DCMs module are connected to the phase counter and the photon counter. Phase counter and photon counter are basically digital counters that provide w_{arr} and p_{cc} generation for tagging the photons detected. Note that the tagging of the photon is equivalent to the mixer operation which is basis of the frequency-domain method. Every time a photon is detected, the trigger line (see Figure 3.1) is activated and the content of the two counters is written into the FIFO block which directly communicates with the USB.

Although this figure is not an accurate reproduction of the new FLIMBox firmware it gives a realistic overview on what is actually inside the instrument. It would be confusing in fact to describe in detail the true RTL circuit schematic – see Figure 3.2.

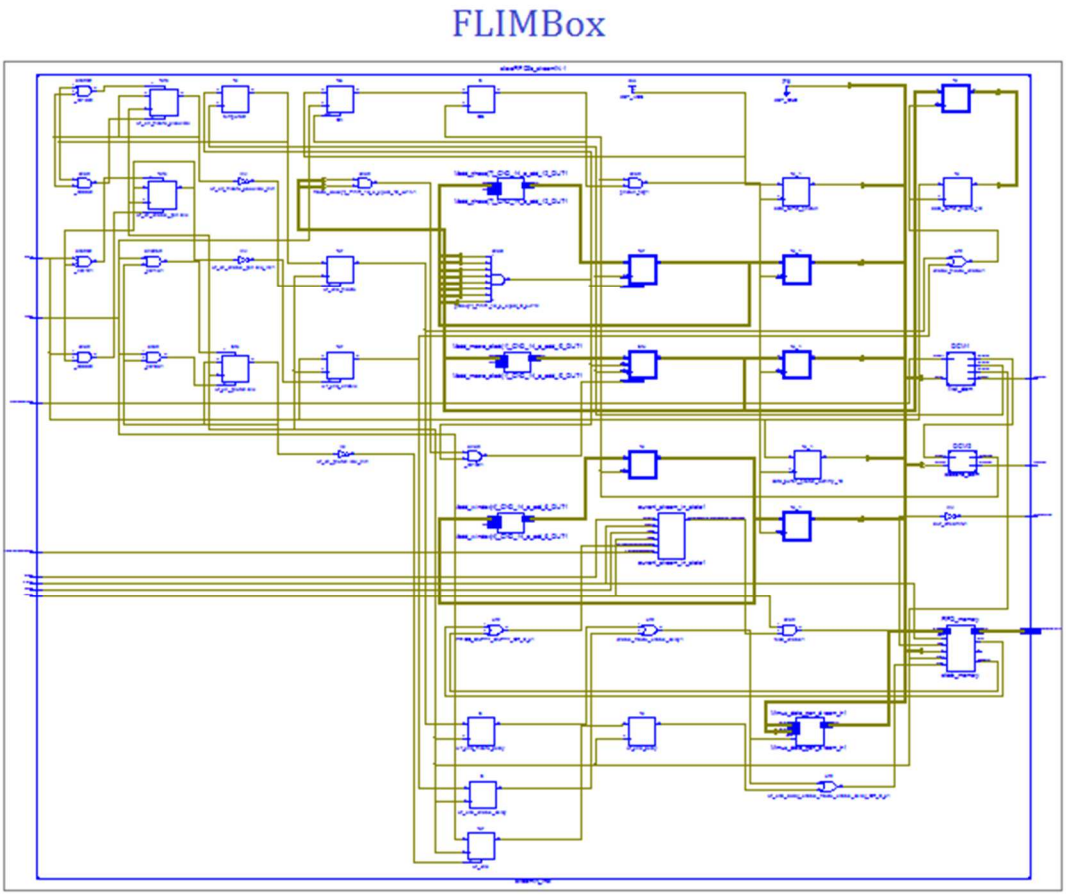

Figure 2.2 – FLIMBox true RTL

In Figure 3.1 and 3.2 we can see the circuit schematic while in Figure 3.3 is possible to see the physical layout of the various components. The card containing the FPGA together with power supply and discriminator (black metal box) is enclosed into a box which can easily be connected to any microscope.

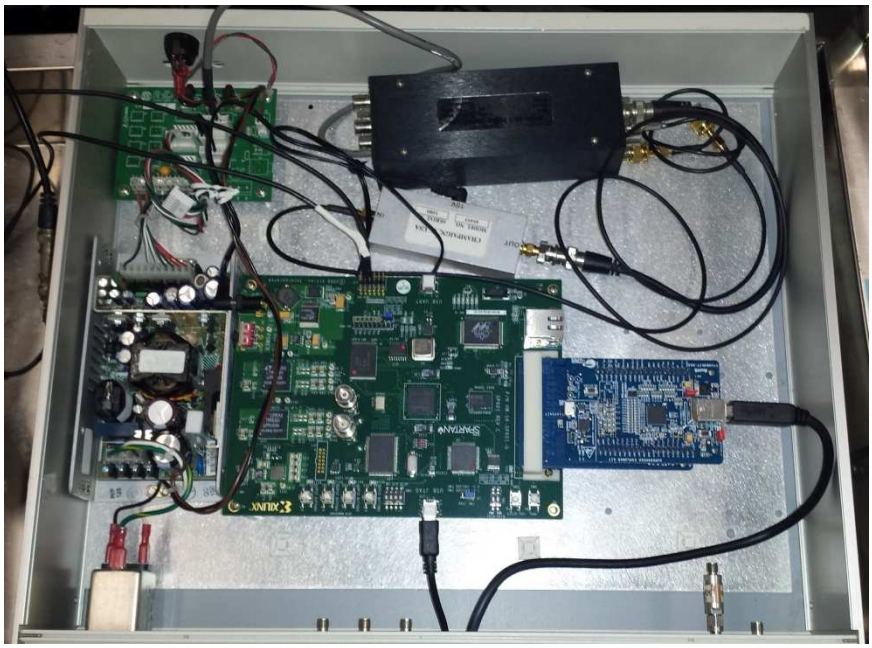

Figure 3.3 – The new FLIMBox

3.2 Frequency response of the new FLIMBox

To determine the frequency response – shown in Figure 3.6 – of the new FLIMBox a constant delay between laser frequency clock signal and photon signal was set, two signal generators were used. One oscillator was use to reproduce the laser frequency at 80MHz and was fed to the clock I/O port of the instrument and to the *trigger* port of the other oscillator for creating a constant delayed signal representing the photons (Figure 3.4), in this way Laser clock and photon were two copies of the same signal but shifted in phase – Figure 3.5.

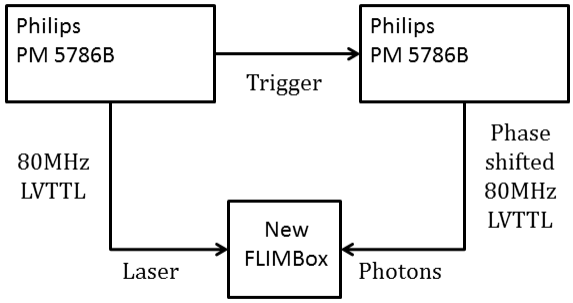

Figure 3.4 – Experimental setup for frequency response characterization

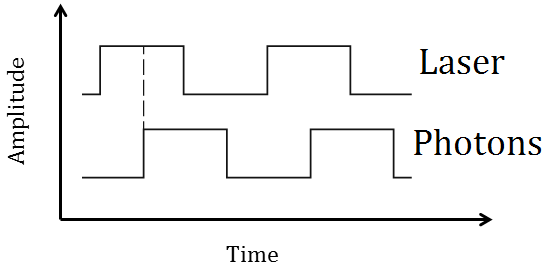

Figure 3.5 – Signals provided as input for frequency response analysis

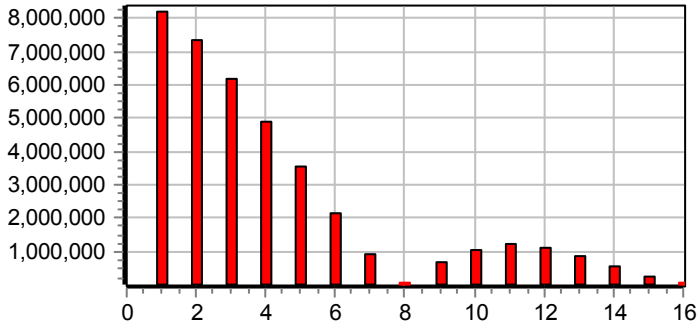

Figure 3.6 – Frequency response of the new FLIMbox for 80MHz harmonics. Intensity value for modulation on the *y* axis and number of harmonic on the *x* axis

This test could not be done with the old FLIMBox because it was impossible to capture and sample photons with a frequency of 80MHz due to the limitations that were

present in the old implementation of the FIFO writing and USB reading speeds. The old FIFO did not allow a flux of photons higher than 12 million counts per second while the new design can capture photons bursts up to 300 million counts per second. Moreover if we compare the newly obtained frequency response with the old FLIMBox we can appreciate the bandwidth improvement of the new design – Figure 3.7.

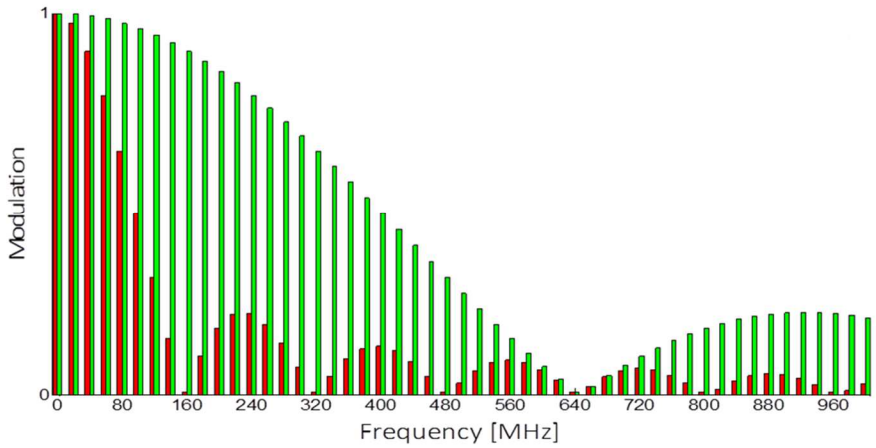

Figure 3.7 – Frequency response comparison between new (in green) and old (in red) FLIMBox designs (harmonics at 20MHz).

Many of the harmonics that are present in the data acquired with the new design are missing or strongly attenuated in data taken with the old FLIMBox.

3.3 Solution measurements

Solution measurements were done to prove FLIMBox integration in various microscope setups and to prove measurements reliability. Test measurements were performed on an 10µM ethanol solution of *Coumarin 6* (3-(2-Benzothiazolyl)-N,N-diethylumbelliferylamine) and a 10µM water solution *Rhodamine 110* (3,6-Diamino-9-(2-carboxyphenyl)xanthylium chloride) as fluorescence lifetime standard. *Coumarin 6* and *Rhodamine 110* have a known lifetime of respectively 2.56 ns and 4.00 ns, their phasor plots are shown in Figure 3.8 and Figure 3.9.

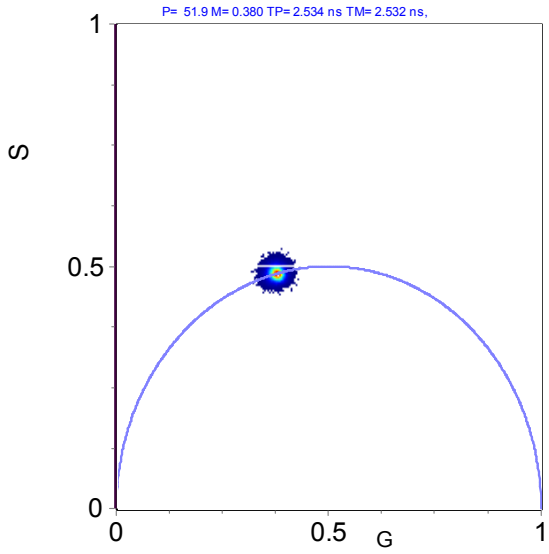

Figure 3.8 – *Coumarine 6* phasor plot τ_p: = 2.534 ns and τ_m = 2.532 ns

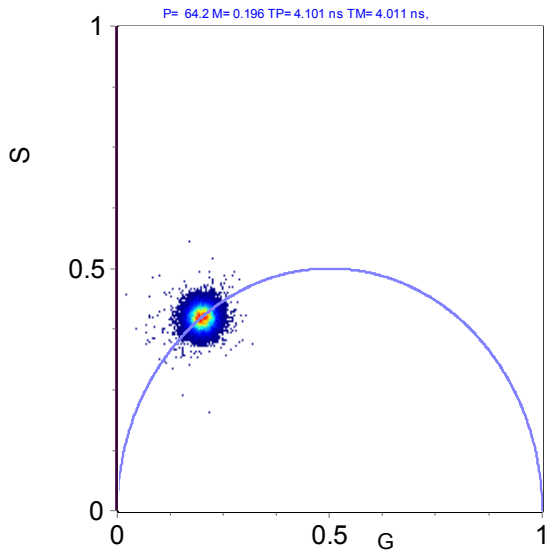

Figure 3.9 – *Rhodamine 110* phasor plot: τ_p = 4.101 ns and τ_m = 4.011 ns

The new FLIMBox clearly produces very accurate data in real situations since it matches the standard for fluorescence lifetime measurements for these two probes. For both probes the measured decay was single exponential and the two independent determinations of the lifetime match within 0.002 ns.

In the next two sections of this chapter we will show the performance of the new FLIMbox for the acquisition of FLIM images. Pixels reconstruction was done by processing the frame-enable signal from the microscope scanner. All the data were elaborated using SimFCS software developed at the LFD.

3.4 *Convallaria majalis* mesurements

Convallaria majalis is commonly used for fluorescence lifetime measurements – Figure 3.10 – 3.11.

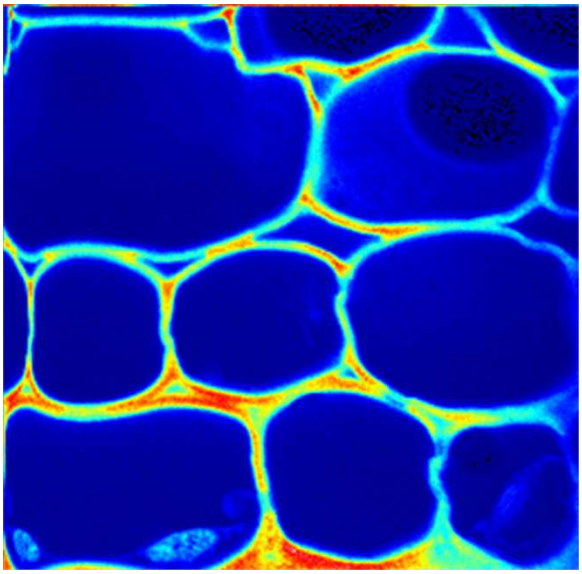

Figure 3.10 – *Convallaria majalis* intensity image (256x256 pixels)

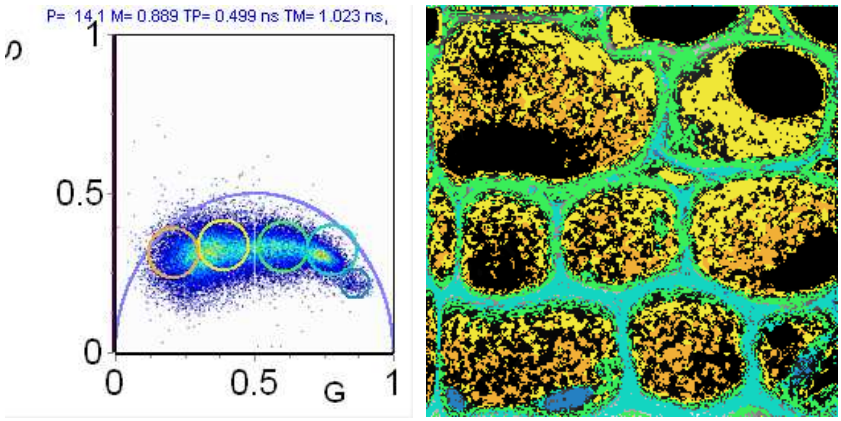

Figure 3.11 – *Convallaria majalis* phasor plot and image painted according to the cursor colors.

The fluorescence of this sample originates from different chlorophylls distributed in different regions of cell wall of the pollen grain and also in some internal organelles. The

analysis of the different regions of the phasor plot is shown in Figure 3.11. In the phasor plot, some specific regions are selected by cursors of different colors. The image at right is drawn with the color of the pixels selected in the phasor plot. This analysis demonstrates the capability to obtain the fluorescence decay in every pixel of the image.

3.5 Urea crystals measurements

Urea crystals generate second harmonic which is a coherent process and consequently has a zero lifetime. Very short lifetimes are generally considered difficult to measure under the microscope. We show in figures images obtained of urea crystals excited at 900 nm with a femtosecond laser – Figure 3.12 and 3.13.

In figure 3.12 we can see the long and bright urea crystals. The phasor plot in figure 3.13 shows a cluster of points at about 0±0.002 ns lifetime. This measurement shows the excellent performance of the new FLIMBox even for the most demanding samples.

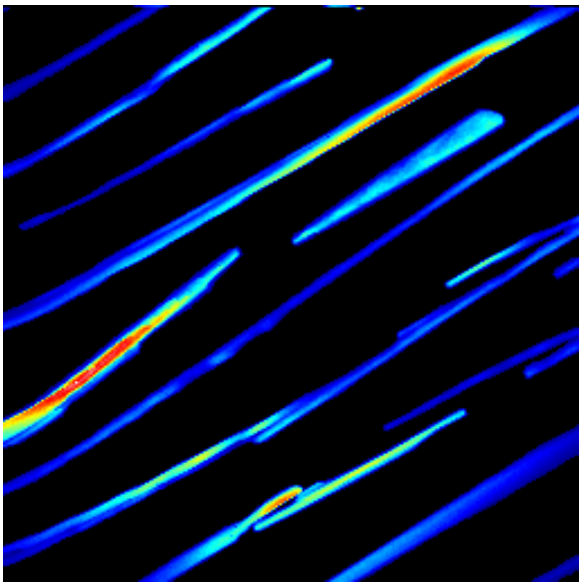

Figure 3.12 – Urea crystals intensity image (256x256 pixels)

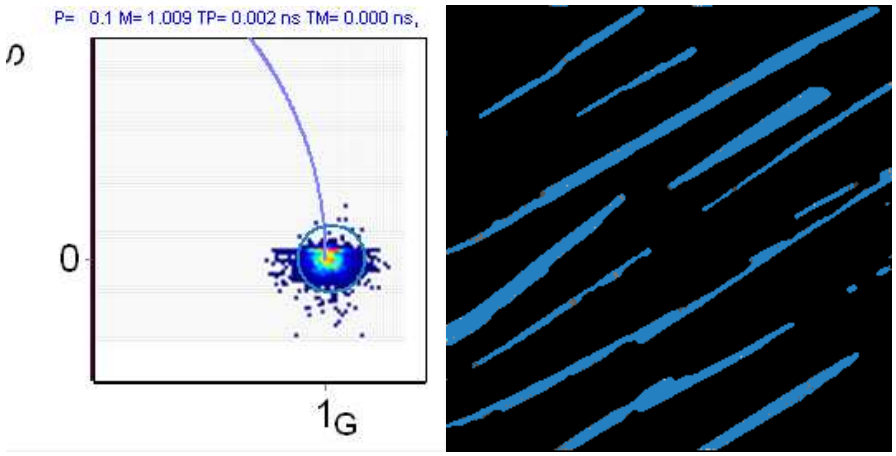

Figure 3.13 – Urea crystal phasor plot: τ_p = 0.002 ns and τ_m = 0.000 ns. Pixels in the image are colored according to the color of the cursors that selects specific pixels in the image

Chapter 4

Conclusion

The development of new generation FLIMBox and its application in microscopy was the main goal of this work. Digital frequency domain approach was applied and modified to achieve higher efficiency together with VHDL circuit implementation. The new device improved significantly the current FLIM frequency domain technology available today. This new design has very low power requirements and a jitter control, has precision and higher frequency capability, and allows the multi exponential analysis to be performed on almost every photon detection based acquisition system (imaging microscopy, FLIM, FCS, tissue imaging).

Based on the results obtained and shown in this thesis, we demonstrated that FPGA-based acquisition systems are a powerful approach for fluorescence lifetime measurements. We simply used digital technology available in the market to implement logics for implementing the digital frequency domain heterodyning principle in a commercial board – Xilinx SP601 together with Cypress FX3. By using the resources offered by the new Spartan-6 and FX3 chips, we overcame the current limit in the maximum count rate in continuous streaming (≈12MHz) and we increased the sampling frequency for the windows in the digital heterodyning method, by designing

this new FLIMBox digital design with improved performance for the determination of fluorescence lifetimes.

The maximum frequency obtained in the FLIMbox is now limited to about 1GHz by the particular chip and technology we are using (Spartan 6, Xilinx). However, faster chips are already in the market. Since the frequency of operation of the FPGA chip is continuously increasing, it is possible that this technology on day will be used for all time domain or frequency domain instruments.

A significant future development of the new FLIMbox design is to implement the VHDL code for a higher performances FPGA chip (such as Virtex or Kintex family – Xilinx). In regard to applications, we envision using this technology for biospectroscopy of tissues, where a high number of photon is available but the high flux cannit be handle by current designs and where the large bandwidth of the new FLIMbox could be fully exploited.

Bibliography

Arnesano, C. (2013). Living in a digital world: features and applications of FPGA in photon detection. LFD - University of California, Irvine.

Becker, W. (2004). Fluorescence lifetime imaging by time-correlated single-photon counting. *Microsc Res Tech*, 58-66.

Colyer, R. A. (2008). Development of a fluorescence lifetime based method to detect and analyze single molecule reactions in solution. LFD - University of Illinois at Urbana-Champaign.

Colyer, R.A., C. Lee, E. Gratton. (2008). A novel fluorescence lifetime imaging system that optimizes photon efficiency. *Microsc Res Tech*, 201-213.

Digman M.A., Caiolfa V.R., Zamai M., Gratton E. (2008). The phasor approach to fluorescence lifetime imaging analysis. *Biophysical Journal*.

Feddersen, B.S.,D.W. Piston, E. Gratton. (1989). Digital parallel acquisition in frequency domain fluorimetry. *Review of Scientific Instruments*, 2929-2936.

Gratton, E. e. (2003). Fluorescence lifetime imaging for the two-photon microscope: time-domain and frequency-domain methods. *Biomed Opt*, 381-90.

Gratton, E., D.M. Jameson, R.D. Hall. (1984). Multifrequency Phase and Modulation Fluorometry. *Ann.Rev.Biophys.Bioeng*, 105-124.

Gratton, E., Dvornikov, A. S., & Crosignani, V. (2014). *Patent No. US8692998.* United States of America.

Gratton, E., et al. (1984). Multifrequency cross-correlation phase fluorometer using synchrotron radiation. *Review of Scientific Instruments*, 486-494.

N.P. Barry, J. Eid, E. Gratton. (2003). Digital heterodyne method for fluorescence lifetime measurements. *Biophysical Journal*, 477.

Robert M. Clegg, Peter C. Schneider. (1996). Fluorescence Lifetime-Resolved Imaging Microscopy: A General Description of Lifetime-Resolved Imaging Measurements. In J. Slavik, *Fluorescence Microscopy and Fluorescent Probes* (pp. 15-33). Springer US.

Spencer, R.D., G.Weber. (1969). Measurements of Subnanosecond Fluorescence Lifetimes with a Cross-correlation Phase Fluorometer. *Annals New York Academy of Sciences*, 361-376.